DYNAMIC BEHAVIOR OF CONCRETE STAVE SILOS

Yasuhiko Sasaki (I)
Jin Yoshimura (II)
Presenting Author: Jin Yoshimura

SUMMARY

Shaking table tests were conducted in three cases using a silo model to investigate the vibration characteristics and the dynamic responses of concrete stave silos during earthquakes. The results demonstrated that the dynamic behavior of the silo model was remarkably dependent on the variety of stored materials, and that the earthquake response characteristics were nonlinear. Furthermore, in order to clarify the restoring force characteristics of stave silos, static loading and earthquake simulation tests were performed using a small-scale silo wall model. These experimental results and a comparison with earthquake response analysis are also described.

INTRODUCTION

Concrete stave silos have been utilized in the U.S.A. and Canada for the past several decades as industrial and agricultural storage facilities for various materials such as coal, grain and silage (Refs. 1, 2). In recent years, stave silos have also been constructed in Japan since they are more economical and reasonable as compared with other types of silos. The cylindrical walls of stave silos are assembled from small precast concrete units called "staves" and held together by exterior adjustable steel hoops. It may therefore be necessary to investigate the dynamic behavior and the earthquake resistance of stave silos with such discontinuous walls.

A series of shaking table tests on a stave silo model was undertaken to examine the vibration characteristics and the earthquake responses of stave silos. Furthermore, static loading and earthquake simulation tests, and earthquake response analysis were carried out using a small-scale silo wall model. The objective of these experiments and analysis was to clarify the static and dynamic restoring force characteristics of stave silos.

SHAKING TABLE TESTS OF 1/6-SCALE SILO MODEL

Stave Silo Model and Experimental Procedures

Based on the law of similitude (Ref. 3), the 1/6-scale stave silo model was designed. The silo model was cylindrically constructed from mortary blocks (26.5 cm x 8.0 cm x 2.2 cm) and steel hoops (5 mm in di-

(I) Research Associate, Dept. of Civil Engineering, Hokkaido University, Sapporo, Japan.
(II) Professor of Civil Engineering, Hokkaido University, Sapporo, Japan.

ameter) on a 2.5 m x 2.5 m shaking table. Each 1.2 m^3 of brown rice and wet sawdust (simulating silage) was used as stored materials. The dimensions of the silo model and the depth of the stored materials are shown in Fig. 1.

Sinusoidal wave excitation and earthquake simulation tests were conducted in three cases of the silo model, respectively. The cases were the model filled with brown rice (Full(BR) model), with sawdust (Full(SD) model) and without the stored materials (Empty model). The earthquake motions used in the experiments were derived from the Nemurohanto-oki (1973), the Tokachi-oki (1968) and the Hidakasankei (1970) earthquake records. Earthquake simulation tests were consecutively carried out in which the peak table motion was gradually increased in the Full(BR) model.

The accelerations of the silo wall and inside the stored materials, the strains of the wall and the steel hoops, the lateral pressures and the shaking table motion were measured. The location of these measured points are also illustrated, using simplified symbols, in Fig. 1.

Experimental Results

The acceleration resonance curves at the top of the model in each case are shown in Fig. 2. These experimental results indicate that the stored materials produce distinct changes in the vibration characteristics, and that the effect of the storage materials is remarkable in the Full(SD) model.

Fig. 3 illustrates time histories of the shaking table acceleration (Nemurohanto-oki), the accelerations at the top (A1) and inside the stored materials (*A4) in the Full(BR) model. Table 1 presents the maximum response values in each case of the model subjected to the Nemurohanto-oki earthquake motion. While the acceleration response at the top (A1) of the Full(SD) model decreases, the maximum response of the Full(BR) model shows the increment of about 40% by comparison with that of the Empty model. From this table, it is also found that the strains of the wall (S3) and the steel hoops (R1, R2, R3) hardly occur at the level of the peak table acceleration in these experiments.

The power spectra of the earthquake responses at the top (A1) and inside the stored materials (*A4) are compared among the each case of the model in Fig. 4. These results indicate that the earthquake response characteristics at the top of the Full(SD) model is quite different from that of the stored material while both characteristics of the Full(BR) model are nearly similar. It is therefore suggested that the dynamic interaction between silo walls and stored materials may be remarkably dependent on the variety of the stored material.

The variations in the response ratios of the Full(BR) model under the Nemurohanto-oki earthquake motions are presented in Table 2. The response ratio here represents the magnitude of each maximum response divided by the maximum table acceleration. From this table, it is found that the earthquake response at the top (A1) showed nonlinear character-

istics, namely, the response ratio decreases gradually from 3.0 to 2.0 as the peak table acceleration is increased. The other results also show that the strain response ratios at the bottom (S3) are nearly constant, and that those of the steel hoops at the top and the bottom (R1, R3) increase from a certain level of the peak table accelerations.

Fig. 5 shows the variation in the maximum lateral pressure distributions of the Full(BR) model under the Nemurohanto-oki earthquake motions. In this figure is also presented the static pressure distribution due to the stored material. The results indicate that the lateral pressure during earthquake motion shifts to a particular distribution with the increase of the peak table acceleration, and that the dynamic pressures at the middle and the bottom (P1, P4) become nearly equal to or exceed the corresponding static ones at the peak table acceleration of 300 gal or over. In these experiments, although several small cracks were observed near joints of the wall, the silo model maintained its normal storage function.

RESTORING FORCE CHARACTERISTICS

Silo Wall Model Experiments

The small-scale silo wall model was constructed from mortary blocks (15.2 cm x 5.0 cm x 2.0 cm) and steel hoops (3 mm in diameter). In order to simulate single degree of freedom system (SDOF system), an iron mass (23.6 kg) was fixed at the top of this wall model. The configuration and the dimensions of the wall model are shown in Fig. 6.

Fig. 7 shows the lateral load-displacement relationship at the top of the wall model under static loading. This result reveals that the wall model has remarkable hysteretic characteristics in which the skeleton curve is a soft-spring type.

The maximum acceleration responses and their response ratios at the top of the wall model subjected to three types of earthquake motions are presented in Table 3. The results show nonlinear response characteristics. Fig. 8 shows the restoring force-displacement curves at certain intervals of time during an earthquake response. From the results, it was found that the wall model during earthquake response also has hysteretic characteristics, which shows a tendency of stiffness degradation as the response amplitude increases. The previous nonlinear response characteristics may be caused by the hysteretic restoring force characteristics.

Earthquake Response Analysis

In general, the equation of motion for SDOF systems under support excitations can be expressed as

$$M\ddot{x} + F(\dot{x},x) = M\ddot{z} \qquad (1)$$

where M = mass of SDOF systems, x = relative displacement with respect to support points, $F(\dot{x},x)$ = nonlinear restoring force characteristics (non-

linear R.F.C.) as a function of velocity and displacement, z = acceleration of support points.

In this analysis, the lateral motions at the top of the wall model were assumed to be that of a SDOF system. The weight of the iron mass including a part of the wall and the resistance of the wall correspond to the mass and the restoring force of the SDOF system, respectively. The load-displacement relationship (Fig. 7) obtained from the static loading test is used as the dynamic R.F.C. of the SDOF system. The equation of motion for this SDOF system may therefore be described as

$$M_e\ddot{x} + R(x) = M_e\ddot{z} \qquad (2)$$

in which M_e = the equivalent mass, R(x) = the hysteretic R.F.C. shown in Fig. 7, $\ddot{z}$ = acceleration of the earthquake motion. Fig. 9 (a), (b) shows a comparison of acceleration responses to the Nemurohanto-oki earthquake motion between the experiment and the analysis. The good agreement indicates that the static R.F.C. of the wall model can be applied to the dynamic ones.

CONCLUSIONS

Based on the results of these experiments and analysis, the following conclusions can be drawn:

1) The stored materials produce distinct changes in the vibration characteristics of stave silos; in general, resonant frequencies become lower and the peak response decreases. However, the degree of the change is remarkably dependent on the variety of stored materials.

2) The relationships of the dynamic behavior during earthquake motions between the wall and the stored materials are also different in accordance with the variety of the materials. The earthquake response results of the Full(BR) model indicated nonlinear characteristics as the peak table acceleration was increased.

3) The wall structures of stave silos show remarkable hysteretic restoring force characteristics in which the skeleton curve is a soft-spring type. The good agreement between the experimental and analytical response results suggests that the dynamic restoring force characteristics may be nearly similar to the static ones.

REFERENCES

1. ACI Committee, "Recommended Practice for Design and Construction of Concrete Bins, Silos, and Bunkers for Storing Granular Materials (ACI 313-77)," American Concrete Institute, Detroit, 1977, pp. 16-18.

2. National Silo Association, "Design Standards for Concrete Stave Farm Silos," July 1974.

3. Emori, I., and Schuring, D. J., "Theory and Application of Model Tests," Gyihodou, Tokyo, May 1973 (in Japanese).

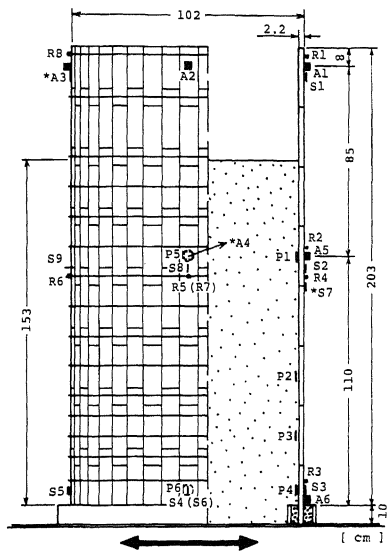

Fig. 1 1/6-Scale Stave Silo Model

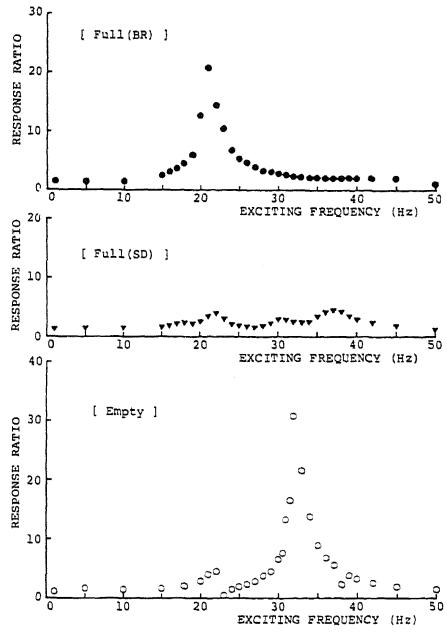

Fig. 2 Comparison of Acceleration Resonance Curves in Each Case of the Model

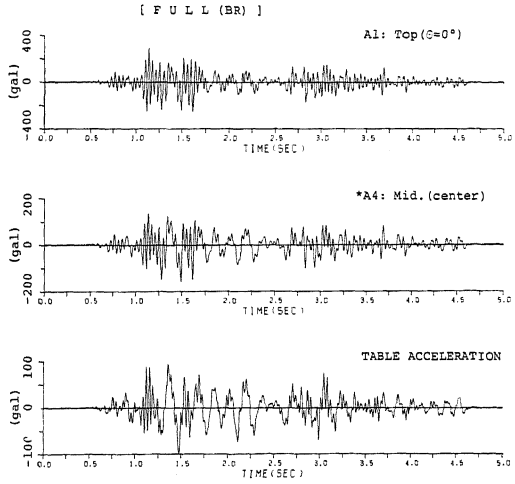

Fig. 3 Typical Time Histories

Table 1 Maximum Response Values in Each Case of the Model

MEASURED POINT	Full(BR)	Full(SD)	Empty
ACCELERATIONS (gal)			
A1: Top(θ= 0°)	294	165	208
A2: Top(θ=90°)	45	41	74
A5: Mid.(θ=0°)	158	126	130
*A4: Mid.(center)	159	389	
TABLE ACCELERATION	98	102	102
STRAINS OF STAVE (μ)			
S3: Bot.(θ=0°)	3.9	1.4	1.1
*S7: Mid.(joint)	17.2	9.5	6.2
STRAINS OF RODS (μ)			
R1: Top (θ=0°)	3.3	8.1	8.2
R2: Mid.(θ=0°)	3.9	4.5	2.8
R3: Bot.(θ=0°)	1.4	1.1	1.2

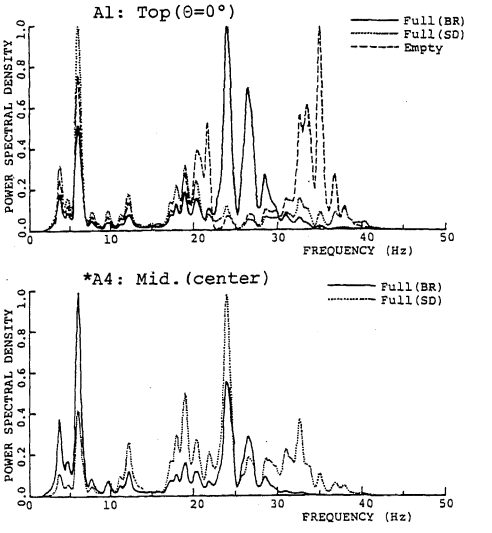

Fig. 4 Comparison of Response Spectra in Each Case of the Model

Table 2 Variations in Response Ratios of the Full(BR) Model

MEASURED POINT	TABLE ACCELERATION (gal) 98	208	308	545
ACCELERATIONS (non-dimension)				
A1: Top(θ= 0°)	3.00	2.82	2.21	1.97
A2: Top(θ=90°)	0.46	0.53	0.70	0.65
*A4: Mid.(center)	1.62	1.48	1.32	1.19
STRAINS OF STAVES (*1/100·μ/gal)				
S3: Bot.(θ=0°)	3.98	3.80	3.83	3.60
*S7: Mid.(joint)	17.6	12.4	10.8	10.9
STRAINS OF RODS (*1/100·μ/gal)				
R1: Top (θ=0°)	3.37	3.99	3.99	7.50
R2: Mid.(θ=0°)	4.39	4.23	4.12	4.07
R3: Bot.(θ=0°)	1.43	5.82	9.25	8.59

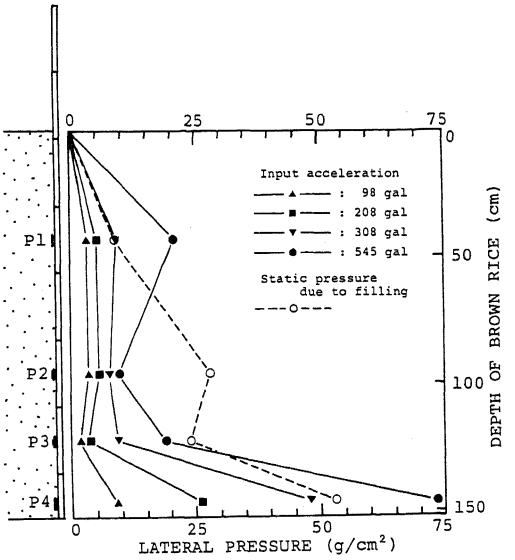

Fig. 5 Maximum Lateral Pressure Distributions in the Full(BR) Model

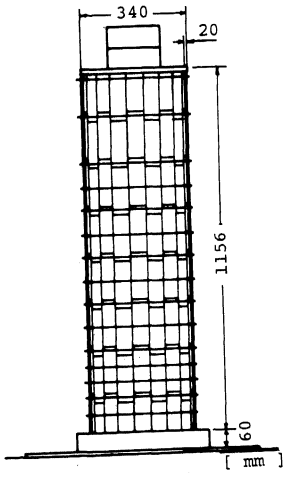

Fig. 6 Stave Silo Wall Model

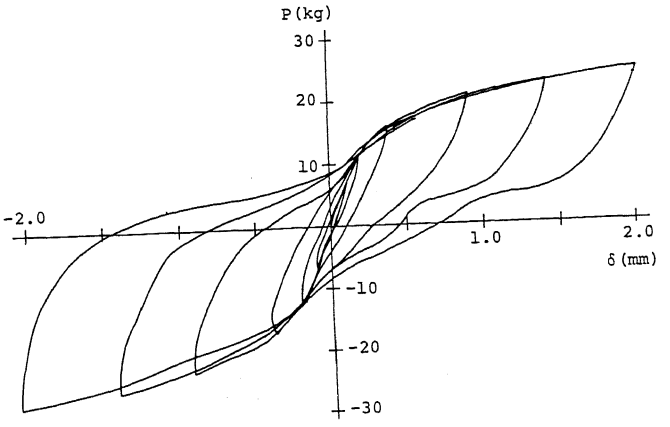

Fig. 7 Load-Displacement Curve under Static Lateral Loading

Table 3 Maximum Values and Response Ratios of Acceleration Response at Top

Type of Earthquake	Max. Table Acc. (gal)	Max. Response Acc. (gal)	Response Ratio
NEMUROHANTO (Akkeshi)	96 229	273 410	2.84 1.79
TOKACHI-OKI (Hachinohe)	100 259	251 443	2.51 1.71
HIDAKASANKEI (Hiroo)	92 264	304 417	3.30 1.58

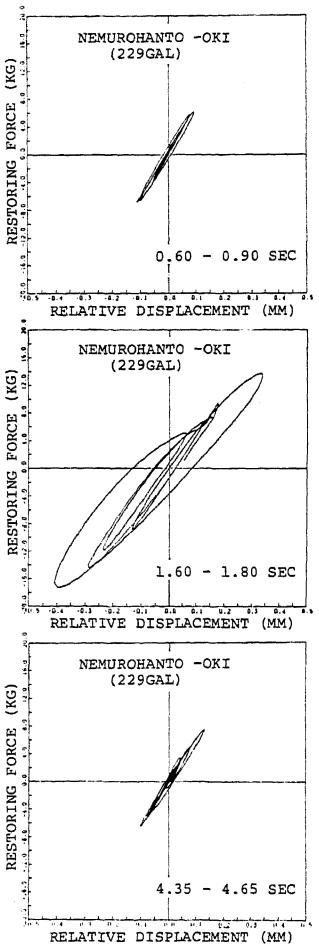

Fig. 8 Restoring Force-Displacement Curves during an Earthquake Response

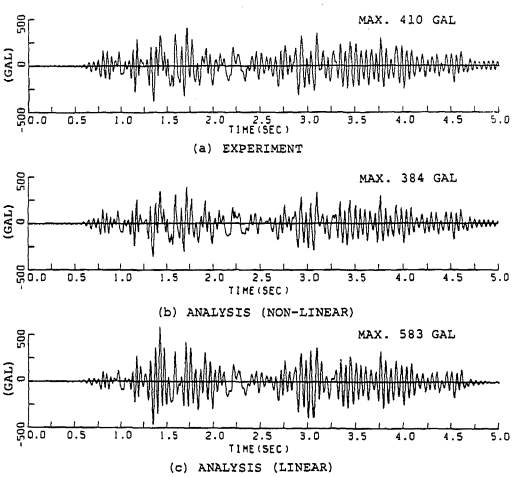

Fig. 9 Comparison of Acceleration Response between Analysis and Experiment